CEOCOR – Copenhagen

21st–24th May 2019

Investigation of pH and oxygen variations on steel electrode under cathodic protection

Federico Martinelli-Orlando, Wei Shi, Ueli Angst

ETH Zürich, Institute for Building Materials (IfB),

ETH Hönggerberg, CH-8093, Zürich, Switzerland

fmartine@ethz.ch

Abstract

Oxygen and pH variations were investigated in continuous cathodic protection (CP) and stray current interferences conditions of steel coupons in water-saturated sandy soil. The aim of this work was to describe the pH evolution and the oxygen concentration at the steel surface under the effect of both conditions.

Carbon steel samples were buried in quartz sands saturated with a simulated soil solution. Oxygen concentration and pH variations were measured by means of planar optical sensors (optodes). Further investigations on the pH variations were performed by means of Iridium Oxides (IrOx) sensors. Electrochemical measurements, i.e. Linear Polarization Resistance (LPR) and potentiodynamic polarization, were conducted to evaluate the corrosion rate of the samples.

The oxygen concentration at the metal surface was found to start decreasing when CP was applied. The dissolved oxygen concentration decreased from 8 to 0 ppm within 30 hours under CP conditions at an E_{on} value of –0.85 V/(Ag/AgCl). On the other hand, an increase in pH at the metal surface to values above 8.5 occurred within only 1 hour after the application of CP, even at low protection current densities around 5 µA/cm^2. Analytical pH measurements were further performed using IrOx sensors positioned in the soil at given distances from the metal surface. In these experiments, a cathodic current density between 10 and 20 µA/cm^2 was used to protect the steel, which lead to pH values around 14.5 measured 5 mm away from the steel surface after 40 hours of cathodic protection.

Although the local pH close to the steel was found to be affected in tests where stray current interferences were introduced, the evaluated corrosion rate was mainly influenced by the average current density that can be calculated from interference current and CP current.

Results for corrosion rates obtained in this study show that pH is a fundamental parameter in protecting the steel.

Introduction

Cathodic protection (CP) is one of the most common and effective techniques to protect steel structures against corrosion [1]. The first attempt of CP dates back to 1824 in the U.K., when Davy attached zinc plates to hulls of military ships to protect copper sheeting by seawater [2]. The first application of CP in soil dates back to 1910 in Germany, when Geppert and Liese developed the idea to protect pipelines from stray current interaction [3, 4]. In 1928 in the USA, Kuhn successfully implemented the CP method to prevent corrosion of buried pipelines [5]. Kuhn first proposed the criterion of -0.85 V/CSE on-potential in 1933 [6]. The protection mechanism, the applicable protection criteria and the corresponding threshold values are still under debate, despite the long and generally successful history of CP [7].

It is well known that steel can be protected by electrochemical polarization. Nevertheless, in the last years, various studies underlined that pH is an important and fundamental parameter for ensuring corrosion protection [1], [7–12]. During CP the residual oxygen present in the soil is consumed and the development of hydroxyl ions at the steel surface provokes the increase in pH in the surrounding of the steel. As soon as the oxygen is consumed the potential of the steel approaches the reversible potential of the hydrogen electrode [1]. Typical values of cathodic current densities in soil are between 0.01-0.5 A/m^2 [13]. Referring to Figure 1 these values correspond to pH-levels from 11-12 [7].

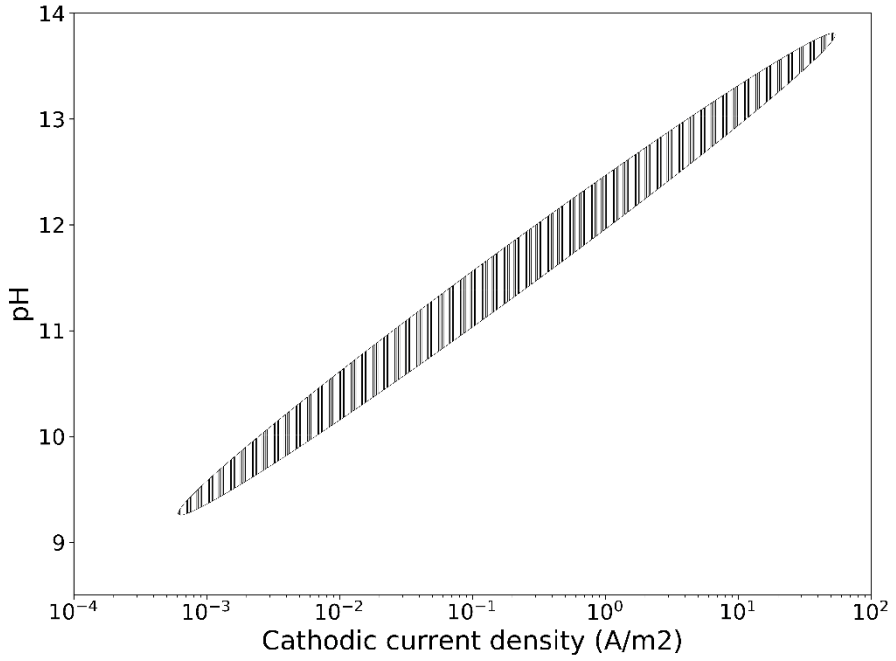

Figure 1: Relationship between cathodic protection density and pH at the steel surface based on data reported and compiled in a published paper [7].

In this study, in situ measurements were performed to evaluate the pH variation in CP condition as a function of protection current density. Considering the example of other civil engineering structures, i.e. reinforced concrete, the pH range of the concrete pore solution is between 12.5 and 13.5. In this alkaline environment, the steel forms a passive layer that lowers the corrosion rate to negligible values. One of the main degradation processes of these structures is called carbonation. Due to the ingress of aggressive species, such as CO_2, the pH of the concrete pore solution is lowered to values where the steel actively corrodes [14]. Therefore, monitoring of pH in such

structure is extremely important. In the last decade, a few innovative sensors have been developed to monitor pH in situ in existing and new structures [15–17].

The aim of this work is to describe the pH evolution and the oxygen concentration at the steel surface under the effect of CP and stray current interference. Iridium Oxide sensors (IrOx) were used in this work in simulated soil to evaluate analytically the pH variations during CP as a function of the distance from the steel surface and the CP application time. Moreover, pH variation and oxygen concentration were also monitored by means of planar optical sensor (optodes) during CP and stray current condition. These sensors were employed to quantify the amount of time that was needed to:

- Increase the pH at the metal surface to alkalinity range in CP condition;
- Consume all the oxygen present in the surrounding of the metal surface in CP condition;
- Return to neutral pH when CP was interrupted.

Corrosion rates were calculated by electrochemical techniques, i.e. Linear Polarization Resistance (LPR) and potentiodynamic polarization.

Materials and Methods

Experimental setup

A three-electrode system was used in this study, Figure 2. The two working electrodes were carbon steel (DIN 1623) embedded in bi-component acrylic resin. The two working electrodes were rectangular (exposed area was 1.19 cm^2 for each); they were positioned in the same plane one next to the other with a gap of approx. 1 mm. They were at all times electrically short-circuited. The soil was composed by quartz sand (0.3-0.9 mm) and a simulated soil solution of composition: 2.5 mmol/L $NaHCO_3$ and 5 mmol/L $Na_2SO_4 \cdot 10H_2O$. The counter electrode was Titanium Metal Mixed Oxide (TiMMO) and it was located 200 mm far from the working electrodes. A Ag/AgCl/sat. KCl reference electrode was placed at 100 mm from the working electrodes. Planar optical sensors (optodes) were placed beside the working electrode surfaces and glued to polymethylmetacrylate container.

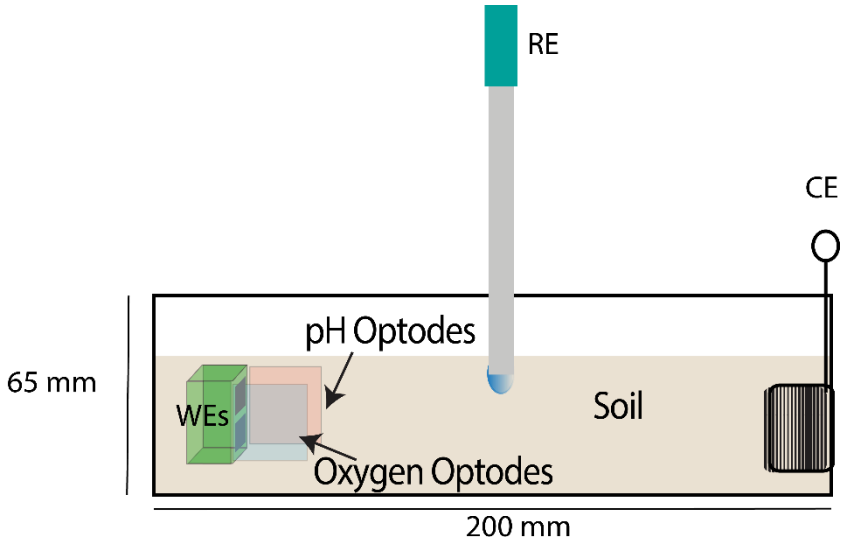

Figure 2: Experimental setup. From left to right: working electrodes (WE), oxygen (blue) and pH (red) optodes, Ag/AgCl sat. KCl reference electrode (RE) and TiMMO counter electrode (CE)

Solartron 1286 electrochemical interface was used to perform all the electrochemical measurements included in this work.

pH and oxygen evaluation during CP

Potential measurements were performed in the laboratory environment at room temperature. After 4 hours of OCP monitoring, CP was applied. The protection level was fixed at a on-potential of – 0.85 V vs Ag/AgCl, corresponding to -0.969 V vs CSE, for 60 hours. It was then followed by at least 4 hours depolarization. The pH and oxygen variations were monitored in all experiments. Figure 3 shows an example of the overall behavior of the potential. Linear polarization resistance (LPR) and potentiodynamic polarization were performed at the end of each experiment.

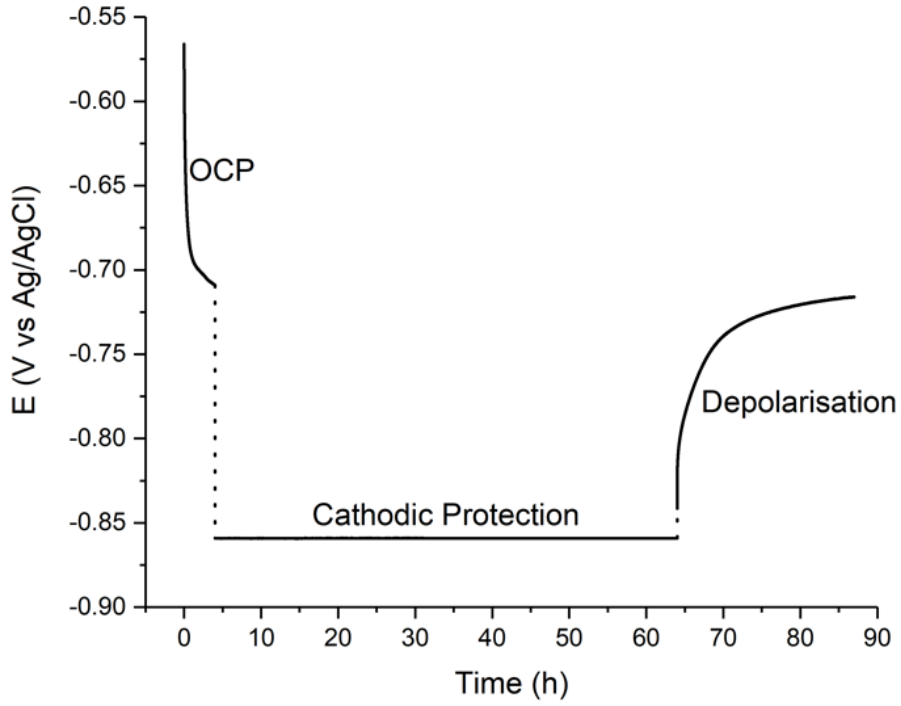

Figure 3: Potential of the WEs variation during cathodic protection experiment in presence of oxygen and pH optodes. Protection level was set to -0.85 V vs Ag/AgCl corresponding to -0.969 V vs CSE.

pH and oxygen evaluation during simulated stray current interference

Potential measurement, together with pH and oxygen observations were also carried out during stray current interference, Figure 4.

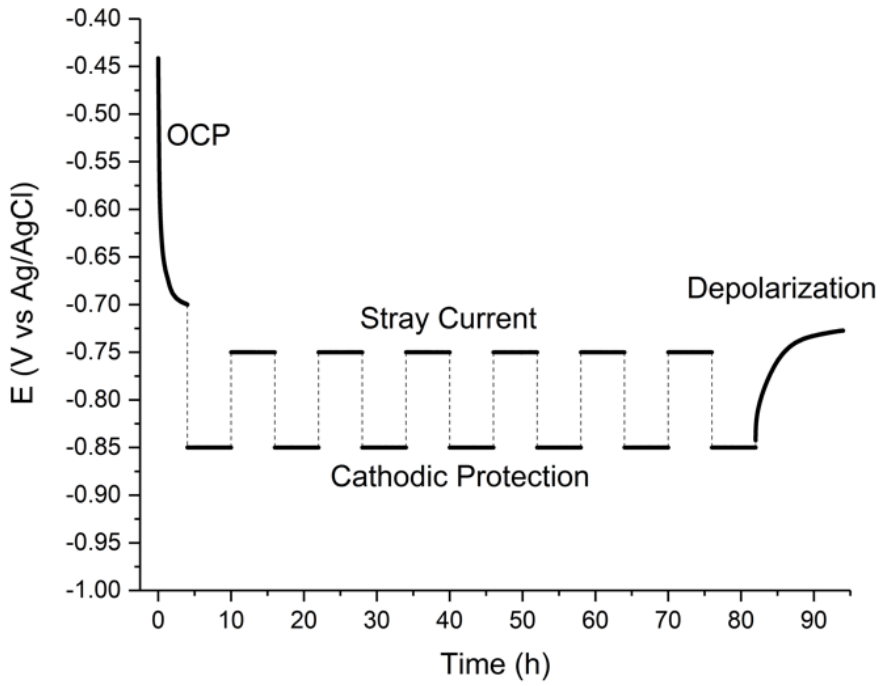

Figure 4: Potential variation during experiment in CP and simulated stray current conditions.

Interference of direct stray current was simulated by polarizing the working electrode in anodic direction to on-potential values of –0.75 V/(Ag/AgCl). 6.5 cycles (12 hours per cycle) were performed after 4 hours of OCP measurements. In other words, the electrode was cathodically polarized for a total of 42 hours and anodically polarized (with an anodic current) for a total of 36 hours. 12 hours OCP measurements were performed during depolarization. In these experiments, only one of the two WEs were connected to the electrochemical circuit. LPR and potentiodynamic polarization measurements were performed in the end (i.e. 94 hours after starting the experiments, or 12 hours after switching CP off).

Iridium Oxides sensor: pH evaluation

Figure 5 gives the topview of the cell and the position of IrOx sensors to measure the pH.

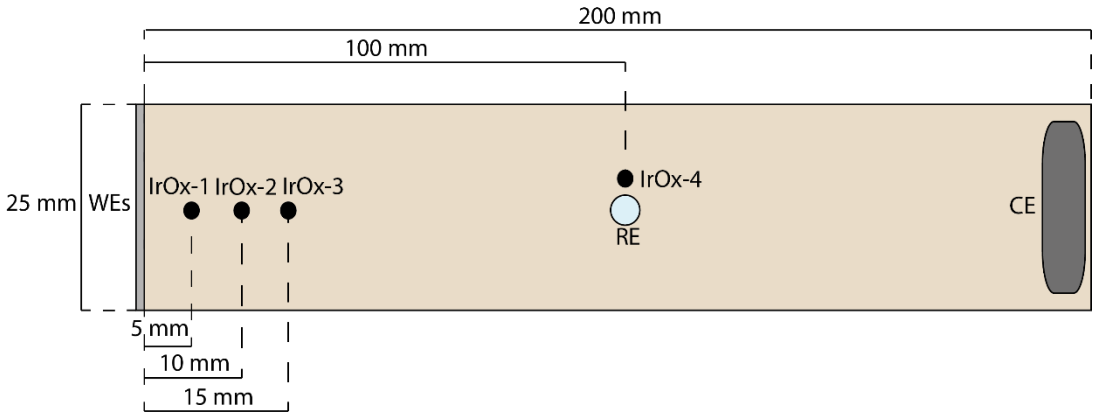

Figure 5: Setup of the experiments involving pH measurement with IrOx sensors.

In this experiment, the pH was observed during cathodic protection. Four parallel carbon steel (DIN 1623) plates were introduced in the setup and embedded in a Teflon sample-holder. Each plate showed an exposed area of 1.25 cm^2. The samples were electrically connected in short circuit.

The counter electrode (CE) was placed at 200 mm from the working electrodes (WEs) and the Ag/AgCl sat. KCl reference electrode (RE) was located at 100 mm from both CE and WEs. The applied on-potential during cathodic protection was -1.1 V vs Ag/AgCl sat. KCl. The experimental time was divided into three parts: 7 minutes of OCP, 60 hours of cathodic protection and 12 hours of depolarization. LPR and potentiodynamic polarization were performed in the end. Keithley 2000 multimeter was used to record the measured potential values between the IrOx sensors and the reference electrode. The values used to calculate the pH have been corrected by removing the ohmic drop.

Optodes calibration

Optodes were used to monitor and evaluate the oxygen content and the pH changes during the experiment. The working mechanism of these sensors is called fluorescence radiomatric imaging (FRIM). Fluorescent chemical dyes are embedded in a polymeric matrix. These dyes react with the environment where the sensor is located in reversible way. When it is subjected to an excitation light (UV), the dyes emit in green and red fluorescence depending on the content of the reacting species in the system [18].

In this study, the pH detectable range of these optodes (SF-HP5R by PreSens) varies between 6.5 and 8.5 pH units. With (SF-RPSu4 by PreSens) the measurable oxygen content varies between 100% to 0% air saturation. Pictures were acquired every 10 minutes. The size of the optodes were 20×20 mm^2. Figure 6 shows the calibration images from pH and oxygen optodes.

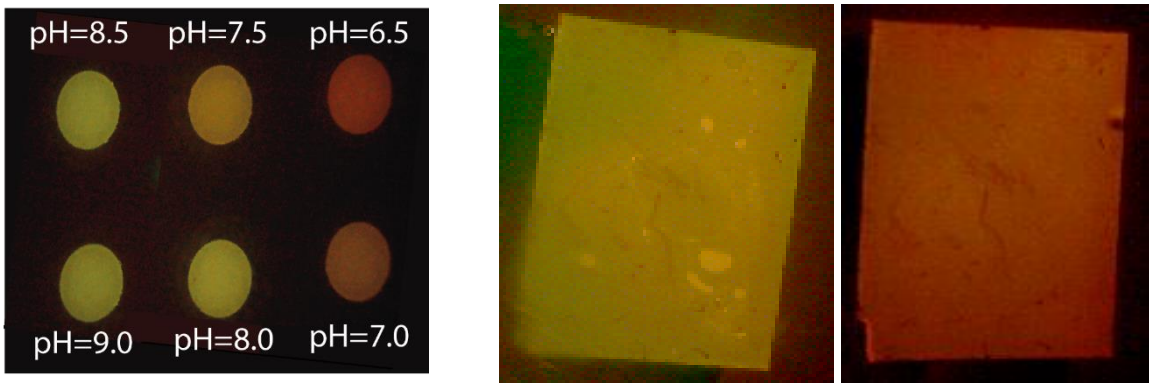

(a) (b)

Figure 6: (a) pH sensor calibration between 6.5 and 9, (b) oxygen sensor calibration showing green in air exposed environment and red in de-aerated condition.

Calibration was performed at the beginning of each experiment. In case of pH calibration, quartz sand with granulometry between 0.3 and 0.9 mm was used in addition to buffer solutions to simulate the subsequent experimental conditions. Instead, for the oxygen optodes calibration a solution of oxygen-free was prepared by adding 1g of sodium sulfite (Na_2SO_3) and 50 µL of cobalt nitrate ($Co(NO_3)_2$) standard solution to 100 mL of H_2O. Deionized water was used as oxygen saturated solution.

Iridium Oxides sensor calibration

Termally oxidized iridium (IrOx) sensors were used to monitor the pH variations during CP and stray current condition. The equilibrium potential of these IrOx sensors at a given temperature depends only on the pH of the solution [16, 17]. Figure 7 shows an example of a calibration curve of a sensor used in the present experiments. The sensors were calibrated in a pH range between 8.5 and 13.5. The calibration was performed one hour before the beginning of each experiment in

simulated soil. Table 1 summarizes the parameters obtained by linear regression of the calibration data.

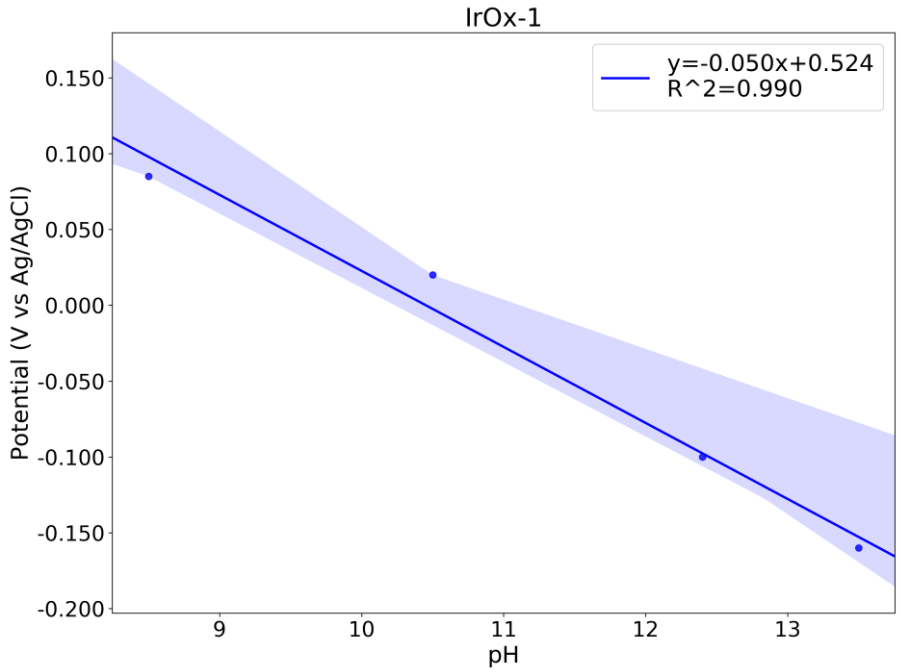

Figure 7: Example of a calibration curve of the IrOx-1 sensor used in this experiment.

Table 1: Parameters obtained by linear regression of calibration data of the four IrOx sensors used in this work.

Sensor	**Slope [V/pH]**	**intercept [V]**	**R^2**
IrOx-1	-0.050	0.524	0.990
IrOx-2	-0.050	0.541	0.981
IrOx-3	-0.050	0.522	0.968
IrOx-4	-0.051	0.557	0.987

Results and discussion

Cathodic protection: pH and oxygen optodes

Figure 8 shows the results for the spatial and temporal distribution of pH and oxygen during application of CP according to Figure 3.

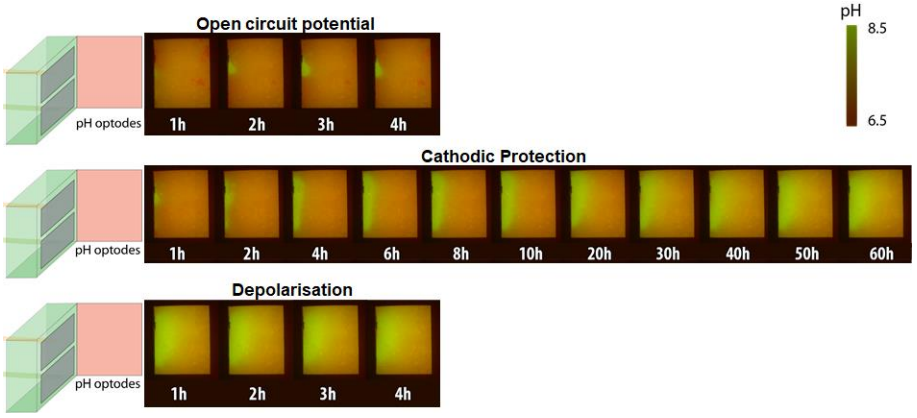

(a)

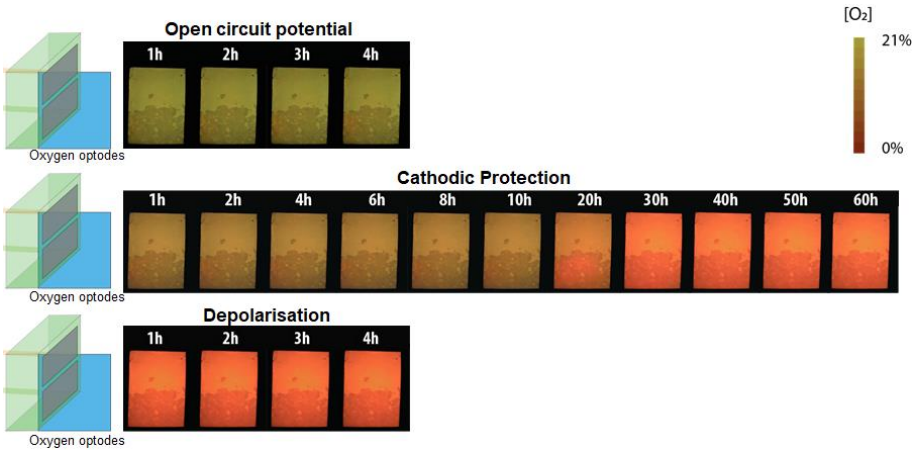

(b)

Figure 8: Temporal and spatial pH (a) and oxygen (b) variation during application of CP. For pH optode green color represents a pH value of 8.5, while red color represents a pH value of 6.5. For oxygen optodes, green color represents 21% air saturation (8 ppm of oxygen dissolved in solution)and red corresponds to 0% air saturation (0 ppm of oxygen dissolved).The dimension of the optodes in this experiment was 20×20 mm^2.The left side of both the optodes is in close proximity of the WEs surfaces evaluating the local pH and oxygen variation until 20 mm from the surface.

Before applying protection current, slight local changes in pH were observed at the location where the two working electrodes meet. This can be explained by galvanic corrosion which occurred due to differential aeration (see distribution of oxygen illustrated by the oxygen optode results in Figure 8(b), with an increasing oxygen concentration towards the upper, air-exposed surface of the sand). The cathodic reaction occurred at the sample closer to the surface; and the anodic reaction was at the sample away from the surface. This explains the local increase in pH only in the region of the upper sample surface.

As soon as cathodic protection was applied to the galvanic element, the pH increased and reached values >8.5 within 2-4 hours at the entire surface of the two working electrodes. With time, this "alkaline front" was found to move out into the soil. The cathodic protection level was kept to –0.85 V vs. Ag/AgCl sat. KCl including ohmic drop (on-potential). The current density varied from

12 μA/cm^2 at the beginning of the CP application to 4 μA/cm^2 after 60 hours. The oxygen concentration was kept decreasing during the experimental time. Within the first 20 hours, the oxygen concentration mainly decreased in the region in front of the lower sample. After 30 hours the oxygen was completely removed from the environment surrounding both working electrodes. This behaviour of the oxygen can be explained by considering that the rate of oxygen consumption during cathodic reactions at the metal surface was faster than the diffusion rate of oxygen in this environment. The diffusion rate of oxygen was not sufficient to maintain a constant supply of oxygen for the cathodic reactions. Nevertheless, the pH at the metal surface was increased to 8.5, even under the condition that oxygen was not abundant, where water reduction reaction acted as cathodic reaction that allowed the pH to increase to a certain level.

When CP was switched off, the oxygen concentration remained in the order of 0 ppm during 4 hours of depolarization. During the same period the pH remained at a value higher than 8.5 at the metal surface.

This experiment showed that the increase in pH occurred within 2 hours from CP application and the pH remained alkaline for at least 4 hours after CP was interrupted. This demonstrated that pH is a parameter that plays a fundamental role in protection mechanism. Considering the last 4 hours of the experiment, it can be seen that the steel was maintained in alkaline pH, theoretically in the passive region of the Pourbaix diagram. This behavior was also supported by the potential variation during depolarization condition. Figure 3 reported that a complete depolarization occurred in more than 10 hours.

Cathodic protection and the effect of stray current: pH and oxygen optodes

Figure 9 shows the pH evolution and the oxygen variation during cathodic protection alternated by stray current interference. In this experiment, only the sample closer to the surface of the soil was connected to the potentiostat. As shown in Figure 9(a), the increase of the pH was observed as soon as the cathodic protection was applied. As reported also in Figure 8, the pH value of 8.5 was reported at the surface of the working electrode within the first 2 hours in CP condition. During stray current interferences, the pH values at the metal surface decreased to neutral values. This behavior showed a repeatability within all the experiments. After 6 hours of depolarization, the pH returned to the neutral values. In this experiment, the pH returned to neutral condition faster than in the experiment with only CP condition. This can be explained by the fact that the alkalinity conditions originated during CP were produced in different time length (6 hours, instead of 60 hours of the previous experiment). Then the alkalinity was removed during stray current interference, because the cathodic reaction was less pronounced in stray current condition and therefore acidic environment was produced. This led to a decrease in pH during stray current interference, but it also reduced the time needed by pH to return in neutral range during depolarization. Indeed, in these conditions it can be assumed that the alkalinity developed during CP had to be, at least partially, recreated from neutral condition every time after stray current interference.

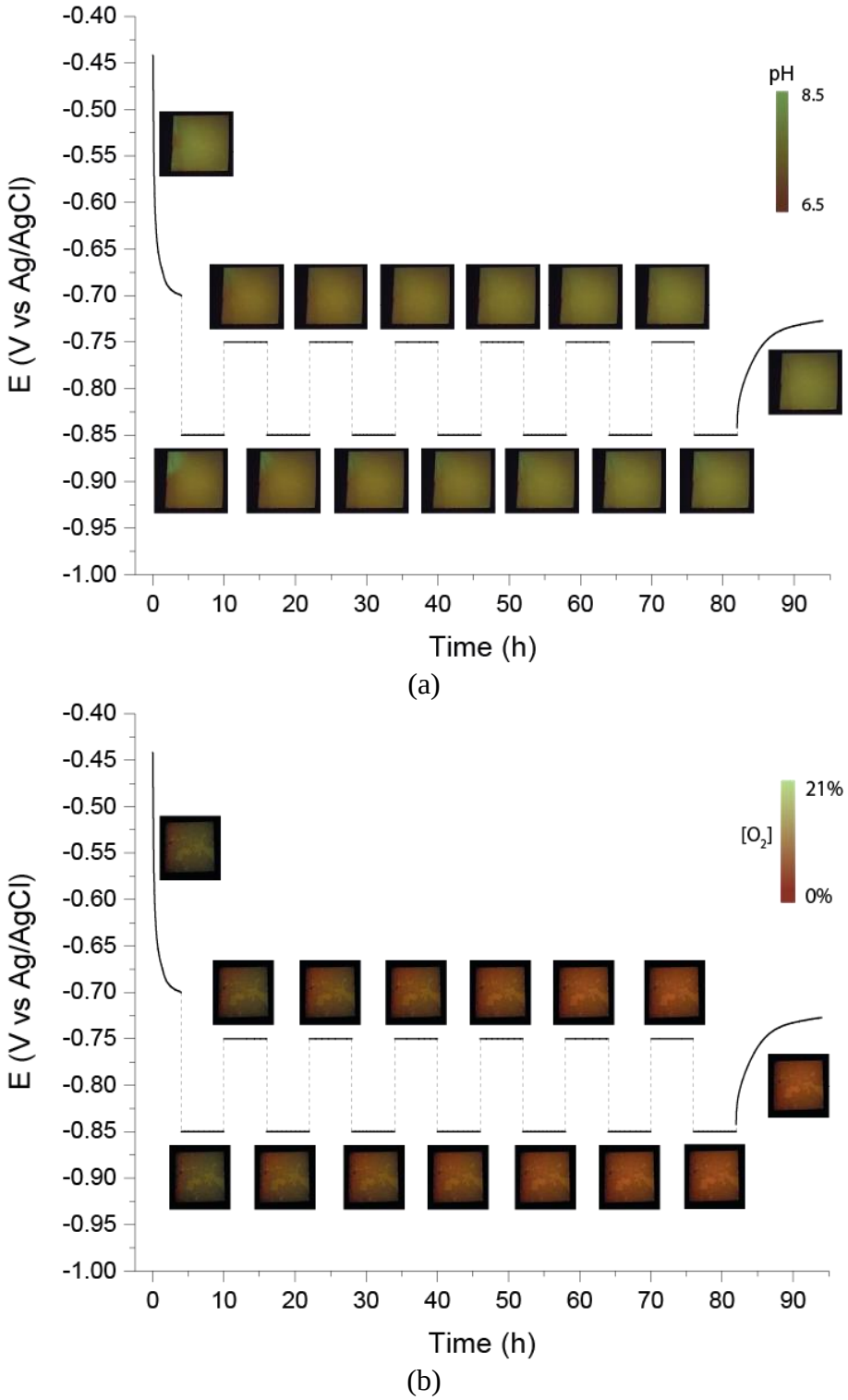

Figure 9: Results obtained by pH (a) and oxygen (b) optodes during stray current interference. The sample was located at the left of the optodes.

Figure 9(b) shows the results obtained by oxygen optodes. The oxygen present in the solution was consumed during both cathodic protection and stray current interferences. All the dissolved oxygen was removed after 30 hours from the beginning of the experiment, which agreed with the observation shown in Figure 8.

Figure 10 shows the behavior of cathodic and anodic current density as a function of the experimental time. The negative and the positive peaks represented the change from cathodic to

anodic and vice versa. The applied current density values were zero at the beginning and at the end during OCP measurements.

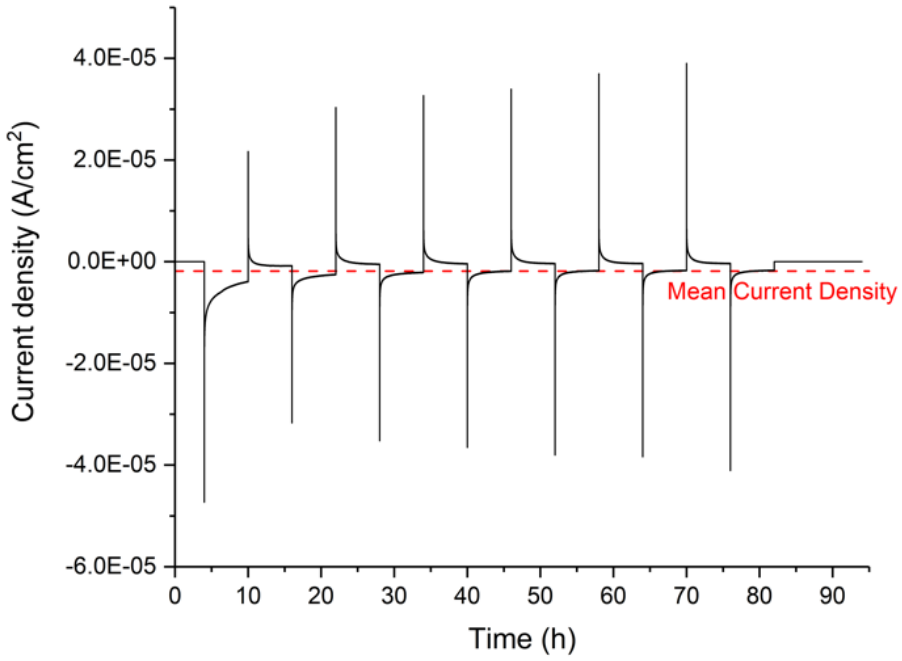

Figure 10: Current density evolution as a function of experimental time. The dashed line corresponds to the mean value of current density calculated over the experimental time.

In Figure 10, the dashed red line represents the mean current density calculated over the entire experimental time. The mean value corresponds to -1.87×10^{-6} A/cm^2 (i.e. -1.87×10^{-2} A/m^2). Thus, the result of the mean current density showed an average slightly cathodic value. During the anodic phases, the average charge flow was about 8.04×10^{-5} C/cm^2

Figure 11 shows potentiodynamic polarization curves obtained at the end of the experiment (IR corrected) and corresponding curve fitting. Tafel slopes, polarization resistance and corrosion rate values were calculated by fitting the experimental data with a method proposed by Mansfeld and Oldham [19, 20]. The polarization resistance value (Rp) was obtained by fitting linearly the surrounding potentials of the OCP (±10mV). Table 2 shows the parameters obtained from curve fitting. I_{corr} represents the corrosion current density in A/cm^2; B_a and B_c are the anodic and cathodic Tafel slopes in V, respectively; E_0 corresponds to the potential at the OCP against Ag/AgCl reference electrode; the corrosion rate is expressed in µm/y; and R^2 is the fitting accuracy.

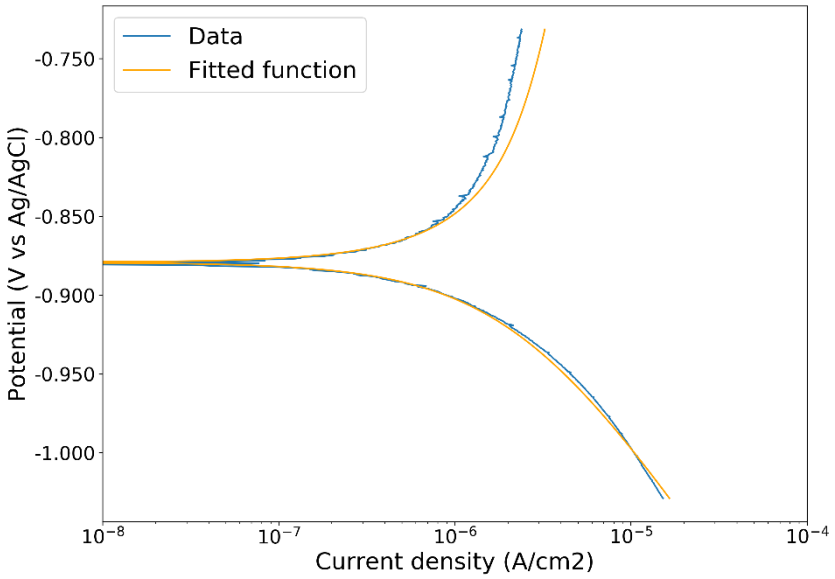

Figure 11: Potentiodynamic polarization of carbon steel sample in simulated soil solution after 6.5 cycles of 6h of cathodic protection and anodic interference followed by 12h in OCP (according to Fig. 4).

Table 2: Parameters obtained by fitting potentiodynamic polarization curves 12 h after switched CP off.

I_{corr} [A/cm^2]	R_p [Ω·cm^2]	B_a [V]	B_c [V]	E_0 [V vs Ag/AgCl]	Corrosion rate [µm/y]	R^2
2.21E-06	26421	0.727	0.164	-0.879	26	0.992

The corrosion rate obtained is 26 µm/y. Together with this low corrosion rate, the R_p value of 26421 Ω/cm^2 and in particular the anodic Tafel slope of 727 mV indicated a passive behaviour of the WE. Similar result was obtained by LPR method performed at the end of the experiment. Table 3 shows the corrosion rate in µm/y and mA/cm^2, and parameters used to calculate them.

Table 3: Parameters and corrosion rate obtained by LPR method 12 h after switched CP off.

Rp [Ω·cm^2]	B_a [V]	B_c [V]	Stern-Geary [mV]	I_{corr} [A/cm^2]	Corrosion rate [µm/y]	R^2
19799	0.727	0.164	54	2.94E-06	34	0.999

Cathodic and anodic coefficients (B_c and B_a, respectively) were extrapolated by potentiodynamic polarization curves. Stern-Geary coefficient was calculated by using Stern- Geary equation [21]. Conversion factor of 11.6 was used to convert corrosion rate from mA/cm^2 to µm/y. For this conversion, the following parameters were used:

- Iron atomic mass = 58.85 g/mol;
- Iron density = 7.87 g/cm^3;
- Iron valence number (n) = 2;
- Faraday constant = 96485 C/mol.

The obtained corrosion rate of 34 µm/y is in the same order of the value calculated by Mansfeld and Oldham[19,20] method. The non-negligible corrosion rates can be related to the time that the working electrode spent in depolarization and in a neutral-range environment. On the other hand, the corrosion rate in the order of 20 µm/y showed that, after 12 hours in depolarisation, the steel was still protected to some extent.

Cathodic protection and Iridium oxides sensors

Figure 12 shows the pH variation during CP condition by means of IrOx sensors. The working electrode was cathodically polarized to an on-potential of –1.1 V vs. Ag/AgCl/sat. KCl for 60 hours.

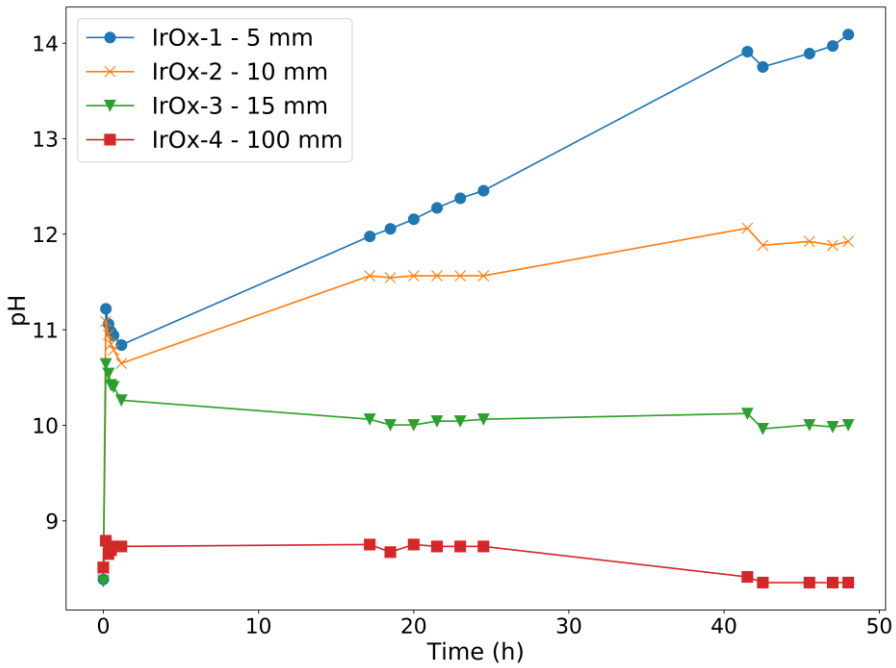

Figure 12: pH values measured with IrOx sensors as a function of time and distance from samples surface during CP condition.

It can be noticed that the pH at the WE surface increases very fast upon CP (which agrees with the observations in Figure 8 and 9). In the first hour of CP application, the measured pH within the distance up to 15mm from the metal surface increased to values above 10.8. The dependence of the pH as a function of the distance from the metal surface was slightly evident in the following 4 hours. At the 18-hour, this dependence is more evident and at the 25-hour it became clear. The pH at 5 mm from the sample surface increased from pH 11, registered in the first hour, to pH 14 after 40 hours. The pH at 10 mm increased for all the duration of the experiment, reaching a pH value of 12 at the end of the experiment. The sensor at 15 mm recorded the first increase to pH 10.8, but in the following hours its pH stabilized to a value around 10. The IrOx-4 was placed next to the reference electrode, at 100 mm away from working electrode. It showed a constant behavior of the pH between 8.2 and 8.8. Even there is some sudden increase registered by all the sensors associated to the presence of the cathodic protection current, the sensors were found stabilized in the presence of the external current after 2 hours.

Figure 13 shows the data obtained by potentiodynamic polarization data. The curve fitting was obtained by using Mansfeld and Oldham method[19, 20]. The polarization resistance value (Rp) was obtained by fitting linearly the surrounding potentials of the OCP (±15mV). I_{corr} represents

the corrosion current density in A/cm^2; B_a and B_c are the anodic and cathodic Tafel slopes in V, respectively; E_0 corresponds to the potential at the OCP against Ag/AgCl reference electrode; the corrosion rate is expressed in µm/y; and R^2 is the fitting accuracy. Table 4 shows the parameter obtained by the fitting. The curves were corrected by the presence of ohmic drop.

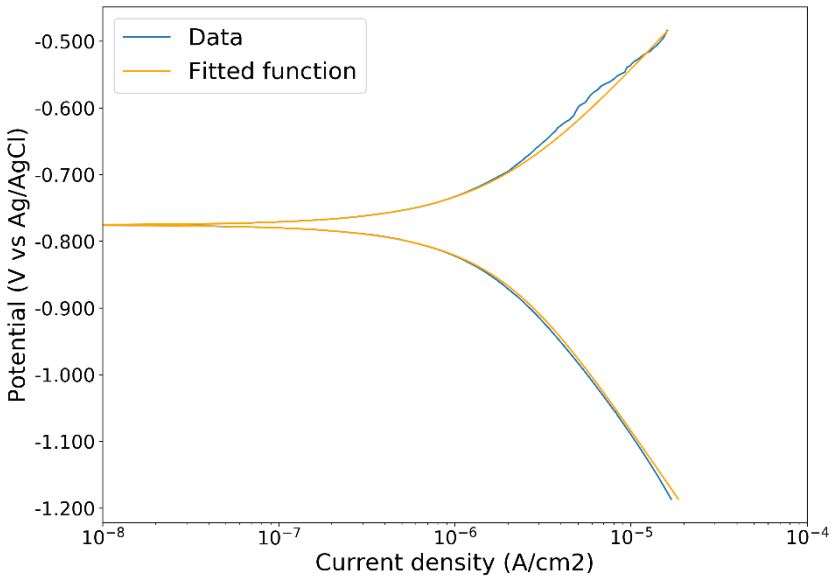

Figure 13: Potentiodynamic of samples after cathodic protection condition.

Table 4: Parameters obtained by fitting potentiodynamic polarization curves 12 h after switched CP off.

I_{corr} [A/cm^2]	R_p [Ω·cm^2]	B_a [V]	B_c [V]	E_0 [V vs Ag/AgCl]	Corrosion rate [µm/y]	R^2
1.62E-06	44483	0.289	0.387	-0.775	19	0.995

The corrosion rate calculated with this method was 19 µm/y. Result in the same order was obtained by LPR method. Table 5 shows the parameters and the corrosion rate calculated by LPR measurement. Cathodic and anodic coefficients (B_c and B_a, respectively) were extrapolated by potentiodynamic polarization curves. Stern-Geary coefficient was calculated by using Stern-Geary equation [21]. Conversion factor of 11.6 was used to convert corrosion rate from mA/cm^2 to µm/y.

Table 5: Parameters and corrosion rate obtained by LPR method 12 h after switched CP off.

R_p [Ω·cm^2]	B_a [V]	B_c [V]	Stern-Geary [mV]	I_{corr} [A/cm^2]	Corrosion rate [µm/y]	R^2
39151	0.289	0.387	72	1.30E-06	15	1.000

The corrosion rate obtained by LPR was in agreement with the one obtained by the potentiodynamic polarization analysis. The results showed a corrosion rate above the threshold of 10 µm/y. Considering that the electrochemical analyses were performed after 12 hours of depolarization, this result can be explained by the time spent in free corrosion condition. Indeed, as registered in the previous experiments, the pH tended to decrease during depolarization condition. Due to the higher polarization level and the higher pH registered in this experiment than

in the previous examples, it was expected that the pH needs more time to return to the neutral range. This can explain the difference in corrosion rates obtained between this and the previous experiments.

Conclusions

Experiments were performed to evaluate pH and oxygen variations during CP condition in simulated soil. The protection level was set to on-potential values of -0.85 V vs Ag/AgCl (-0.969 V vs CSE) and -1.1 V vs Ag/AgCl (-1.219 V vs CSE). Corrosion rates 12 hours after switching CP off were obtained by electrochemical techniques.

With the results gained from this study it is possible to draw these major conclusions:

- The time needed to increase the pH above 8.5 (recorded by optodes) at the steel surface during cathodic protection with on-potential of -0.85 V vs Ag/AgCl was lower than one hour. With the protection level at an on-potential of -1.1 V vs Ag/AgCl, the increase of pH to values above 11 was recorded by iridium oxides sensors (IrOx) as soon as the CP was applied.
- At the CP on-potential of -0.85 V vs Ag/AgCl the complete removal of oxygen at the steel surface occurred within the first 4 hours from the time when CP was applied.
- At the tested on-potential of -0.85 V vs Ag/AgCl, the pH needed between 6 and 10 hours to return to neutral value upon switching CP off. The oxygen concentration, instead, remained around 0 ppm for at least 12 hours upon switching CP off.
- During anodic stray current interference (with an average charge flow of 8.04×10^{-5} C/cm^2), the pH was neutralized within 6 hours.
- 12 hours after switching CP off (after application of both on-potentials of -0.85 V vs Ag/AgCl and -1.1 V vs Ag/AgCl), corrosion rates were measured in the order of 20 µm/y, indicating that the previous polarisations had still some protective effects.

References

[1] U. Angst *et al.*, 'Cathodic protection of soil buried steel pipelines - a critical discussion of protection criteria and threshold values: Protection criteria for cathodic protection of steel pipelines', *Mater. Corros.*, vol. 67, no. 11, pp. 1135–1142, Nov. 2016.

[2] H. Davy, 'VI. On the corrosion of copper sheeting by sea water, and on methods of preventing this effect; and on their application to ships of war and other ships', *Philos. Trans. R. Soc. Lond.*, no. 114, pp. 151–158, 1824.

[3] R. Juchniewicz, J. Jankowski, and K. Darowicki, '8 Cathodic and Anodic Protection', p. 88.

[4] W. von Baeckmann, W. Schwenk, W. Prinz, and W. von Baeckmann, Eds., *Handbook of cathodic corrosion protection: theory and practice of electrochemical protection processes*, 3rd ed. Houston, Tex: Gulf Pub. Co, 1997.

[5] J. Kuhn, 'Galvanic Current in Cast Iron Pipes, Their Causes and Effects, Methods of Measuring and Means of Prevention Paper presented at Bureau of Stds', presented at the Soil Corr. Conf. Washington, DC, 1928.

[6] R. J. Kuhn, 'Cathodic protection of underground pipe lines from soil corrosion', *Proc Am Pet. Inst*, vol. 14, pp. 153–167, 1933.

[7] M. Büchler, U. M. Angst, and B. Ackland, 'Cathodic protection criteria: a discussion of their historic evolution', presented at the EUROCORR 2017 (European Corrosion Congress), 2017.

[8] F. Kajiyama and K. Okamura, 'Evaluating Cathodic Protection Reliability on Steel Pipe in Microbially Active Soils', *CORROSION*, vol. 55, no. 1, pp. 74–80, Jan. 1999.

[9] A. Brenna and P. di Milano, 'Can an Intermittent Cathodic Protection System Prevent Corrosion of Buried Pipeline?', p. 11.

[10] A. Junker, R. Denmark, and P. Møller, 'AC Corrosion and the Pourbaix Diagram', p. 15.

[11] A. Brenna, P. di Milano, and V. Mancinelli, '5721: Effects of Intermittent DC Stray Current on Carbon Steel Under Cathodic Protection', p. 12.

[12] B. Gummow, 'An Alternative View of the Cathodic Protection Mechanism on Buried Pipelines', p. 12.

[13] R. W. Revie, *Corrosion and corrosion control: an introduction to corrosion science and engineering*. John Wiley & Sons, 2008.

[14] L. Bertolini, B. Elsener, P. Pedeferri, E. Redaelli, and R. B. Polder, *Corrosion of steel in concrete: prevention, diagnosis, repair*. John Wiley & Sons, 2013.

[15] Y. Femenias, U. Angst, F. Moro, and B. Elsener, 'Development of a Novel Methodology to Assess the Corrosion Threshold in Concrete Based on Simultaneous Monitoring of pH and Free Chloride Concentration', *Sensors*, vol. 18, no. 9, p. 3101, Sep. 2018.

[16] R.-G. Du, R.-G. Hu, R.-S. Huang, and C.-J. Lin, 'In Situ Measurement of Cl^- Concentrations and pH at the Reinforcing Steel/Concrete Interface by Combination Sensors', *Anal. Chem.*, vol. 78, no. 9, pp. 3179–3185, May 2006.

[17] Y. Seguí Femenias, U. Angst, and B. Elsener, 'Monitoring pH in corrosion engineering by means of thermally produced iridium oxide electrodes', *Mater. Corros.*, vol. 69, no. 1, pp. 76–88, Jan. 2018.

[18] H. Stahl, A. Glud, C. R. Schröder, I. Klimant, A. Tengberg, and R. N. Glud, 'Time-resolved pH imaging in marine sediments with a luminescent planar optode: pH imaging in marine sediments', *Limnol. Oceanogr. Methods*, vol. 4, no. 10, pp. 336–345, Nov. 2006.

[19] K. B. Oldham and F. Mansfeld, 'Corrosion rates from polarization curves: A new method', *Corros. Sci.*, vol. 13, no. 10, pp. 813–819, 1973.

[20] F. Mansfeld, 'Tafel slopes and corrosion rates from polarization resistance measurements', *Corrosion*, vol. 29, no. 10, pp. 397–402, 1973.

[21] D. Matthews, 'The Stern-Geary and related methods for determining corrosion rates', *Aust. J. Chem.*, vol. 28, no. 2, p. 243, 1975.